Accepted Manuscript

Title: Material Flow During Friction Stir Welding of Ti-6Al-4 V

Author: Paul D. Edwards M. Ramulu

PII: S0924-0136(14)00484-1
DOI: http://dx.doi.org/doi:10.1016/j.jmatprotec.2014.11.046
Reference: PROTEC 14210

To appear in: *Journal of Materials Processing Technology*

Received date: 26-7-2014
Revised date: 25-10-2014
Accepted date: 28-11-2014

Please cite this article as: Edwards, P.D., Ramulu, M.,Material Flow During Friction Stir Welding of Ti-6Al-4<ce:hsp sp=Ö.25Ï>V, *Journal of Materials Processing Technology* (2014), http://dx.doi.org/10.1016/j.jmatprotec.2014.11.046

Material Flow During Friction Stir Welding of Ti-6Al-4V

Paul D. Edwards[1,2,a], M. Ramulu[2,b]

[1]The Boeing Company, P.O. Box 34787 MC 5A-39, Seattle WA 98124 USA

[2]University of Washington, Dept. of Mechanical Eng. Box 352600, Seattle WA 98195 USA

[a]paul.d.edwards2@boeing.com, [b]ramulum@u.washington.edu

Keywords: Friction Stir Welding, Titanium, Material Flow.

Abstract. 6 mm thick Ti-6Al-4V butt joints were produced with a tracer material embedded in the joint under a variety of process conditions, namely rotational speed and traversing speed, in an attempt to relate the welding process parameters to the material flow behavior via post weld radiographic and metallographic evaluations. It was found that by embedding refractory alloy powder into the joint line, welding through it, and subsequently x-raying the joint, the material flow patterns could be examined. The tracer material was distributed over a wider area in the weld zone relative to its starting position, implying a fair amount of mixing occurred even though little vertical movement of the tracer material was observed. There was minimal effect of material flow patterns as a function of welding parameters observed using the tracer material and radiographic examination, but defect formation in the root, where there was no tracer material, examined by cross sectional metallographic evaluations were found to be dependent on the rotational speed and traversing speed conditions. Lack of penetration defects were generally associated with relatively "cold" welding conditions (low rotational speed/high traversing speeds) and voids with "hot" conditions (high rotational speed/low traversing speeds).

Introduction

Friction Stir Welding (FSW) is becoming a commonly used joining process for materials such as aluminum, copper, steel and more recently, titanium. Over the course of its development, extensive studies have been performed on the metallurgy and mechanical properties of the welds. Mishra and Mahoney (2007) have provided one of the most compreshensive single sources of literature on Frictoin Stir Welding and Processing, throughly summarizing much of the work that had been done to date. In these studies, where microstructures are evaluated, or mechanical properties are characterized and related back to microstructures, assumptions are often made with respect to the peak welding temperatures and material deformation, or mechanical work, during the process. Assumptions are made about these aspects of the process because of difficulties associated with experimentally measuring them and their key influence on the resulting metallurgical and mechanical properties.

Limited literature is available on experimental evaluations of the temperatures and material flow during the FSW process. Temperature measurements have been successfully made by embedding thermocouples into the weld zone and stirring through them, capturing the temperature profile at a as the weld tool approaches until the thermocouples are consumed in the stir zone. In some cases, the thermocouples continue to collect data even after the weld tool has passed. Several researchers, such as Tang et al. (1998), have measured the temperature distribution during FSW of Aluminum. Tang et al. (1998) measured the temperatures in the weld as a function of the distance from the centerline of the weld, the rotational speed and traversing speed. Edwards and Ramulu (2010) were the first to use this method of embedding thermocouples to experimentally measure the temperatures in the weld zone durring FSW of Titanium.

Material flow during FSW is possibly one of the most difficult aspects of the process to explicitly characterize experimentally. Metallographic analysis can be performed after welding and based on the resulting weld microstructure conclusions can be drawn about the temperatures and deformation in the weld zone during the process. However, metallographic analysis after welding only provides information about the end state and doesn't necessarily define the deformation history resulting in that end state. Furthermore, it can be difficult to decouple the effects of weld temperature and deformation via post weld metallographic analysis alone. The thermocouple technique can be used to isolate the weld temperature variable, but assessing the material flow behavior during FSW is still necessary to understand the process in its entirety.

To visualize the flow of material during the FSW process a tracer technique can be used. This is done by embedding a foreign material in the work piece that can withstand the temperatures and forces during processing and be detected by a non-destructive inspection method or metallographic examination upon being stirred by the FSW tool. Colligan (1999) used strips of steel shot beads along the longitudinal direction of the joint at various depths and distances from the weld centerline in aluminum work pieces. After welding, the work piece was examined by x-ray to determine the final location of the markers and define the material flow behavior. The tracer material nearest the shoulder is subjected to the largest degree of displacement. Deeper in the weld, farther away from the influence of the shoulder, the tracer material is deposited more uniformly behind the tool.

Seidel and Reynolds (2001) and Guerra et al. (2005) also used methods similar to Colligan (1999) in order to visualize the material flow during FSW of aluminum. Seidel and Reynolds (2001) embedded markers into the work piece at various locations and upon completion of the weld, the work piece was progressively machined down from the top surface and at each stage was etched and metallographically examined. Guerra et al (2005) used strips of Copper in an Aluminum work piece and x-ray post inspection to visualize the material flow. Seidel and Reynolds (2001) observed that the bulk of the material in the weld nugget is simply moved around the pin and left directly behind the tool relative to its original position. Actual stirring of the martial was only observed in the top of the weld where influenced by the tool shoulder. Generally there was orderly material flow that followed streamlines. Some vertical movement was seen due to the threaded pin geometry used in welding of aluminum alloys. Seidel and Reynolds (2001) noted that the material seemed to be extruded around the pin of the tool and then forged under the shoulder of the tool once it is deposited behind the pin. Other FSW material flow experiments included Schneider (2007) who used wire marker materials to follow the weld zone material deformation. It was found that material entering the weld zone on the retreating side was extruded around the pin while material on the advancing side was stirred around the tool before being deposited behind. Li et al. (1999) welded dissimilar alloys together in order observe metallographically how the two materials mixed together. Schmidt et al. (2005) performed CT scans of welds to visualize the flow of tracer material in the weld zone in 3-dimensional images as opposed to 2-dimensional x-rays or metallographic sectioning. Several researchers, such as Arbegast (2008), have attempted to develop analytic and numeric models of the material flow during FSW to help with understanding the process and optimizing the welding parameters to avoid defect formation, such as voids and lack of penetration, which are directly associated with the material flow behavior.

Since the tool geometries and material properties are different in FSW of titanium compared to aluminum, the material flow observations made in aluminum FSW are not necessarily directly applicable to titanium. More information is becoming available on the process parameters, microstructure, and mechanical properties of titanium FSW's (e.g. Edwards and Ramulu, 2010). However, virtually no work has been published relative to the thermomechanical behavior of the process. A previous study (Edwards and Ramulu, 2010) was conducted on the temperatures during

FSW of titanium as a function of the process, but *no studies on material flow in titanium FSW have been performed to date*. The purpose of this research is to document the weld zone material flow behavior in titanium FSW and attempt to determine the effect of weld parameters, such as rotational speed and traversing speed, on material flow and defect formation.

Experimental Set up and Procedure

The material used in this investigation was 6 mm thick Ti-6Al-4V titanium alloy plate. The chemical composition for this material is nominally 6.28% Al, 0.1% C, 0.21% Fe, 0.010% N, 0.13 O, 4.05% V, with Ti as the balance. The tracer material used was a tungsten (W), 25% rhenium (Re) blend powder 20 micron in size. Re and W have densities roughly 5 times that of Ti-6Al-4V, which is one of the main reasons they were selected as the powders to embed in the Ti workpiece. After welding, these higher density materials will provide large contrast with the matrix material in radiography. Tungsten also doesn't chemically react with, or dissolve into, Ti even at elevated temperatures, (Frary et al. 2003).. Furthermore, the room temperature tensile strength of pure W is 400 MPa with an elongation of 30% as reported (Yih, 1990). Pure Re has strength of 1130MPa and an elongation of 24% (Grobstein, 1990). Based on previous research by Edwards and Ramulu (2010), in the weld zone of a Ti FSW during the process, peak temperatures are approximately 1000C and flow stresses are in the range of 100MPa. At 1000C, the strength of W is 250MPa. Based on the high strength at temperature and high melting point of the powder materials relative to the Ti FSW processing temperatures and flow stresses, and also lack of reactivity between W/Re and Ti, it is not anticipated that the powder material will melt, react with the Ti base material, or be severely deformed during processing. Deformation of the powders could have an influence on the subsequent radiographic imaging, but because large deformations are not anticipated and is expected to be minimal (Klopp, 1968), particularly at the resolutions desired for this study. Further investigation may be required regarding this issue though.

All materials were machined along the abutting edges that would be subsequently welded together. After machining, parts were chemically etched to remove any contaminates prior to welding. Two 100 mm wide by 300 mm long plates were welded together to make 200 mm wide by 300 mm long welded panels. A 1.25 mm wide x 1.25 mm deep x 76 mm long pocket was milled into the center of one piece along the edge to be welded, Figure 1. The pocket was then filled with the W-Re powder tracer material. The edge of the other piece to be welded was left flat, with no pocket milled into it. Since the tracer material would only be on one side of the joint in the pocket, in most cases, the weld tool was offset 0.625 mm (half of the total tracer pocket depth) from the weld seam centerline to the side of the joint that contained the tracer material so that the center of the tracer material pocket would be aligned with the center of the weld tool. For two trials, the weld tool was offset from the tracer material pocket centerline, one weld in each direction, in order to place the tracer material on either the advancing or retreating side of the weld. Even though the weld plates were approximately 300 mm in length, only 175 mm long welds were made. This was done to stop the weld within the portion of the joint that contained the tracer material. By stopping the weld before all of the tracer material was stirred, post weld inspection would show the relative starting position of the tracer material, along with its flow around the tool, relative to where it is deposited in the weld.

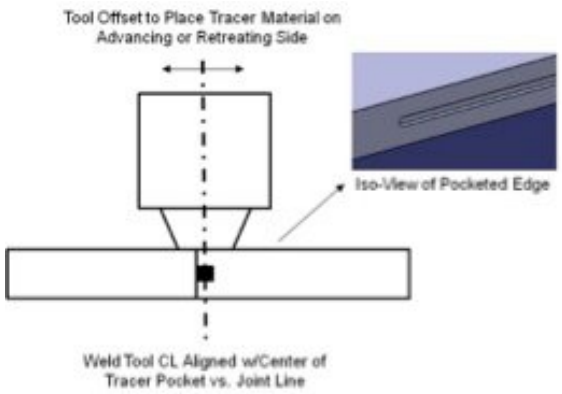

Figure 1 Schematic of Edge Prep for Tracer Material and Weld Tool Positioning.

The weld parameters used for this study were based on previous work (Edwards and Ramulu, 2010). Using a parameter set of 300 RPM rotational speed at a 100 mm/min traversing speed as the baseline condition, welds were also made with rotational speeds of 200 RPM and 400 RPM, and traversing speeds of 50 mm/min and 100 mm/min. All welds were made with a 3 degree back tilt, where the tool was tilted 3 degrees away from the direction of travel. The FSW welding tool used was a tungsten lanthanum (W-La) alloy with a 25 mm diameter shoulder and a pin that tapered from 20 mm in diameter at the shoulder to 10 mm at the tip over a 5.9 mm pin length. All welds were made on a W-La backing anvil. Thermal management via internal water cooling the pin tool and anvil were also utilized. All welds were made in z-axis position control and for each weld responses such as plunging force, travel load and torque were measured using sensors built into the welding machine. The tool tilt, shoulder engagement and pin tip to anvil ligament were held constant for all trials. A test matrix of conditions used in these experiments is given in Table 1. The location of the tracer material pocket with respect to the weld tool centerline is defined as follows; CL identifies that the tracer material was aligned with the centerline of the tool and Ret/Adv identify when the tracer material was aligned with either the advancing or retreating sides of the tool centerline.

Table 1 Summary of parameters used for material flow experiments.

Weld #	Rotational Speed (RPM)	Traversing speed (mm/min)	Tracer Location
1	300	100	CL
3	400	100	CL
4	300	50	CL
5	300	150	CL
6	200	100	CL
8	300	100	Ret
9	300	100	Adv

After welding, the location of the W-Re tracer material in the weld was determined by 2-D digital radiography (x-ray), 3-D radiographic Computerized Tomography (CT) scans and metallographic analysis. The 2-D x-rays were used to determine the material flow patterns when viewed from the top of the weld. CT scans were performed in an attempt to obtain 3-dimensional material flow visualization and determine if any through thickness material flow was occurring. Metallography was performed on weld cross sections to examine through thickness material flow and to determine if there were any defects that could be correlated to the process parameters and material flow.

The x-ray images were taken with a Viscom 225 kV micro-focus X-ray generator and a 16 bit Perkin Elmer XRD1621AN digital detector array. The X-ray beam was set to 100kV and 1600 micro-seconds. Placing the X-ray tube at 48 inches from the detector and the coupon placed mid-way between the tube and the detector, a 2X geometric magnification was produced. The image is comprised of 80 frames @ 250 milliseconds each. It is typical with digital detector arrays to take multiple fames which are averaged to significantly increase the image contrast sensitivity. The CT data was captured using a North Star Imaging M500 X-Ray/CT imaging system. The reconstruction was performed using the EFX-Ct 1.2 Software. The reconstruction model was based on 540 views taken at 2 frame's per second with 4 frame's averaged. A Fein Focus 225 X-Ray tube supplied the power and a Varian 2520 detector panel captured the data. The approximate voltage used was 220kV and the current was approximately 300mA. These 540 views were geometrically reconstructed into a 3 dimensional representation.

Results

A weld made at the baseline parameter set of 300 RPM rotational speed and 100 mm/min traversing speed is shown in Figure 2. The plunging force (z-force), travel load (x-force) and torque are given along with a photograph of a typical weld surface and an x-ray of that same weld. The ramp up of forces at the beginning of Figure 2 a, from time = 0 to approximately time = 01:50, are associated with the plunge of the tool into the material before the traverse down the weld joint line begins. For this weld, the process loads are relatively consistent and stable resulting in a weld surface that is smooth and uniform. The top view x-ray shows that the W-Re tracer material (showing white in x-ray image) entering the joint on the centerline is deposited in a single line behind the tool, slightly to the advancing side of the joint.

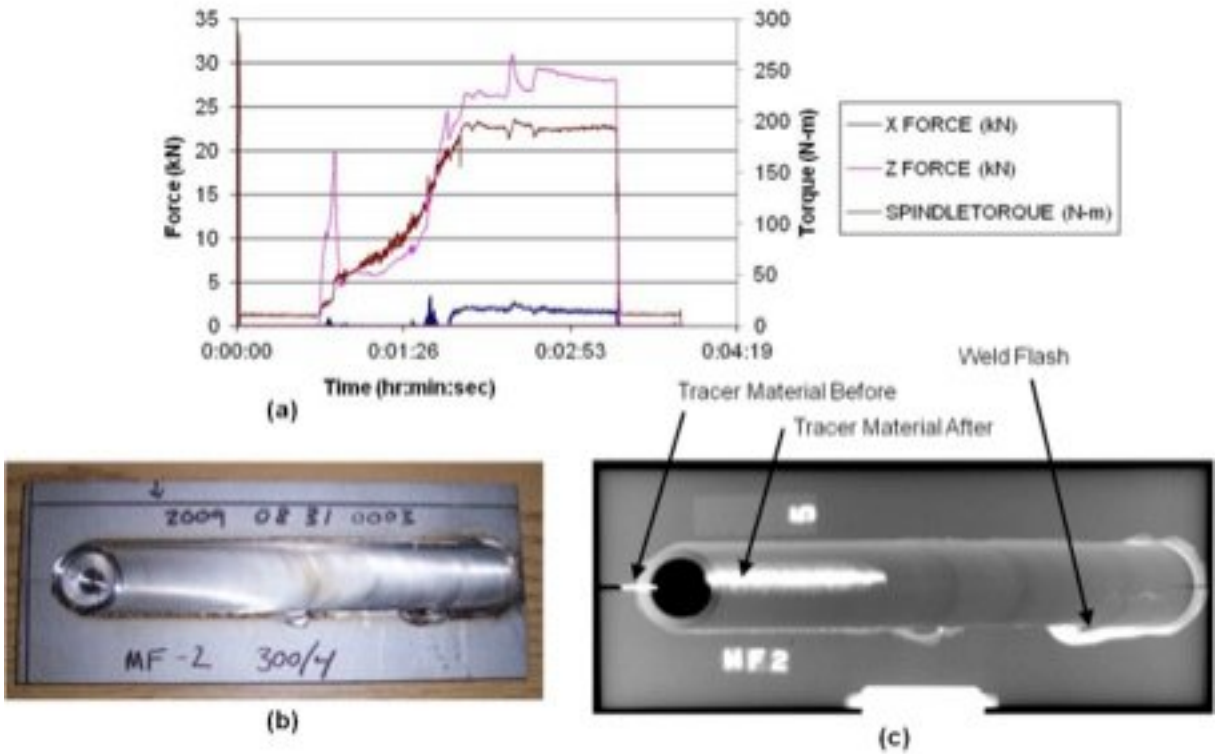

Figure 2 Results from center point weld condition, 300 RPM at 100 mm/min. a) Weld forces, b) weld surface and c) 2-D x-ray.

X-rays of welds made at rotational speeds between 200 and 400 RPM and traversing speeds from 50 to 150 mm/min are given in Figure 3 a and arranged as a function of the process conditions they were produced at with rotational speed (RPM) on the vertical axis and traversing speed on the horizontal axis. As with the material flow seen in the baseline condition of 300 RPM and 100 mm/min (Figure 2), all the weld conditions took the incoming tracer material, passed it around the retreating side of the pin and deposited it behind the tool, slightly to the advancing side of the weld. In all cases the distribution of tracer material behind the pin tool appears to be contained to a fairly tight band implying a lack of extensive or randomized mixing. The lowest traversing speed condition resulted in the greatest spread of the tracer material across the width of the nugget behind the tool. Figure 3 b shows the material flow pattern recorded with 3-D radiographic Computerized Tomography (CT) scans at the same process conditions the x-ray images in Figure 3 b. Similar to the x-ray results, the CT scans showed no significant influence of weld parameters on tracer movement.

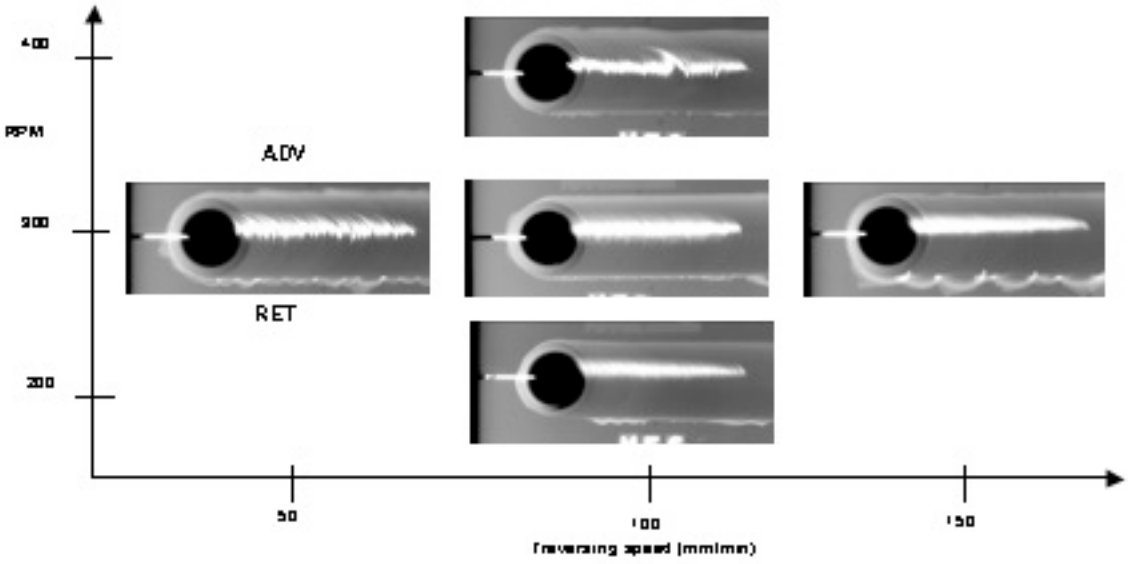

(a)

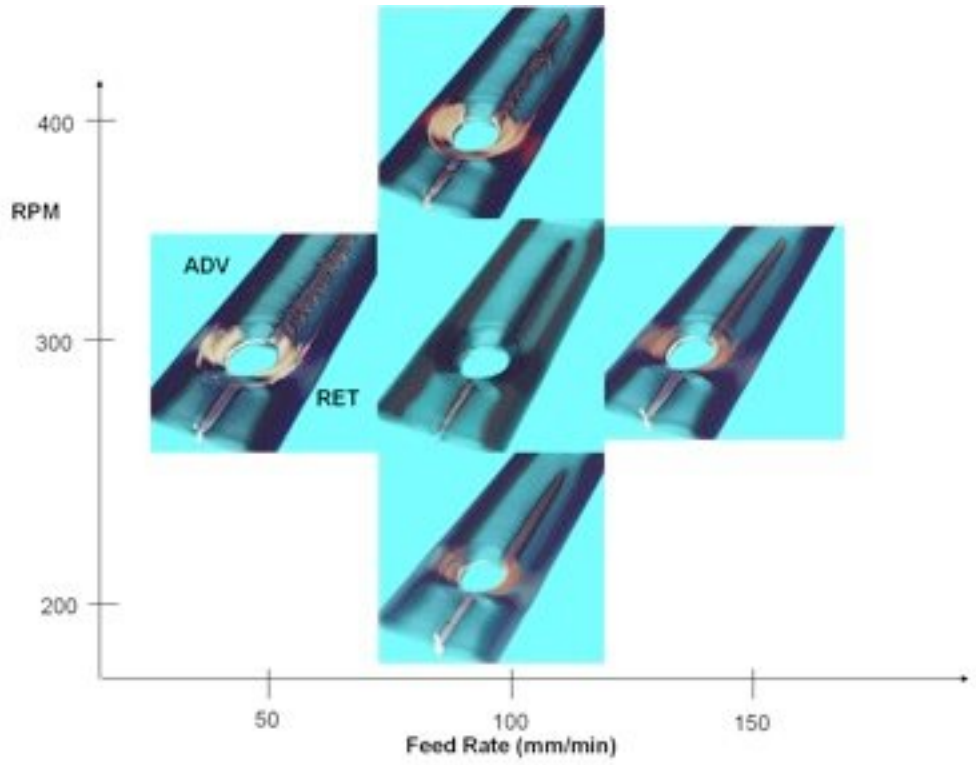

(b)

Figure 3 Material flow patterns as a function of parameters shown by a) x-ray and b) CT scan**.**

The plunging forces for each of these welds is given in Table 2. Increasing rotational speed and decreasing traversing speed result in decreased loads. Rotational speed appears to be the primary driver for plunging force within this range of parameters tested as the 200 RPM rotational speed resulted in the highest plunging force and the 400 RPM rotational speed the lowest load.

Table 2 Experimentally measured plunging forces as a function of FSW process parameters.

Rotational Speed (RPM)	Traversing speed (mm/min)	Plunging force (kN)
300	50	22-24
300	100	26-29
300	150	36-40
200	100	53-62
400	100	15-18

In addition to determining how the material entering the weld zone at the centerline of the joint was transferred around and deposited behind the pin, it is also necessary to examine how material entering on either sides of the weld centerline, also known as the advancing and retreating sides, move. Figure 4 shows x-rays for welds made with the tracer material entering on the advancing and retreating side of the weld. Material entering on the advancing side travels around the pin and is deposited over a wider span and even farther to the advancing side from where it started. The tracer material starting on the

retreating side is also moved around the pin of the tool and spread across a wider span than started, all farther towards the advancing side of the weld

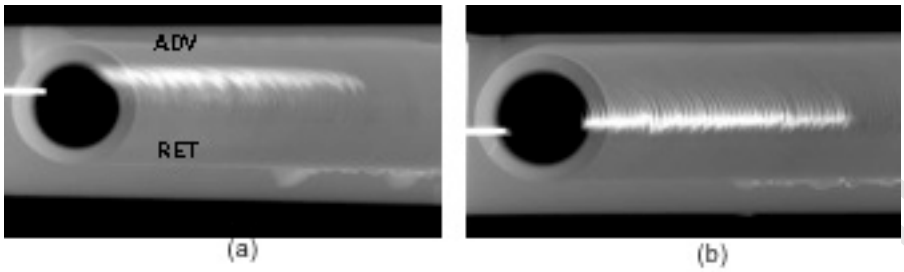

Figure 4 Two dimensional x-rays of welds with tracer material starting on the a) advancing and b) retreating side of the weld centerline. Tool rotation is counter clockwise.

Figure 5 shows the 3-D CT scan from a weld made at 300 RPM and 150 mm/min. Figure 5 also shows a 2-D cross section of the 3-D CT scan data taken parallel to the welding direction at the weld centerline and a 2-D plan view at the depth of the weld where the tracer material was present. These images show where the FSW tool was retracted from the weld zone and how the tracer material enters the weld zone, sweeps around the tool and is deposited behind the tool. Only minimal downward material flow is observed. The dashed appearance of the tracer material behind the tool in the 2-D cross section parallel to the welding direction is associated with the weld pitch.

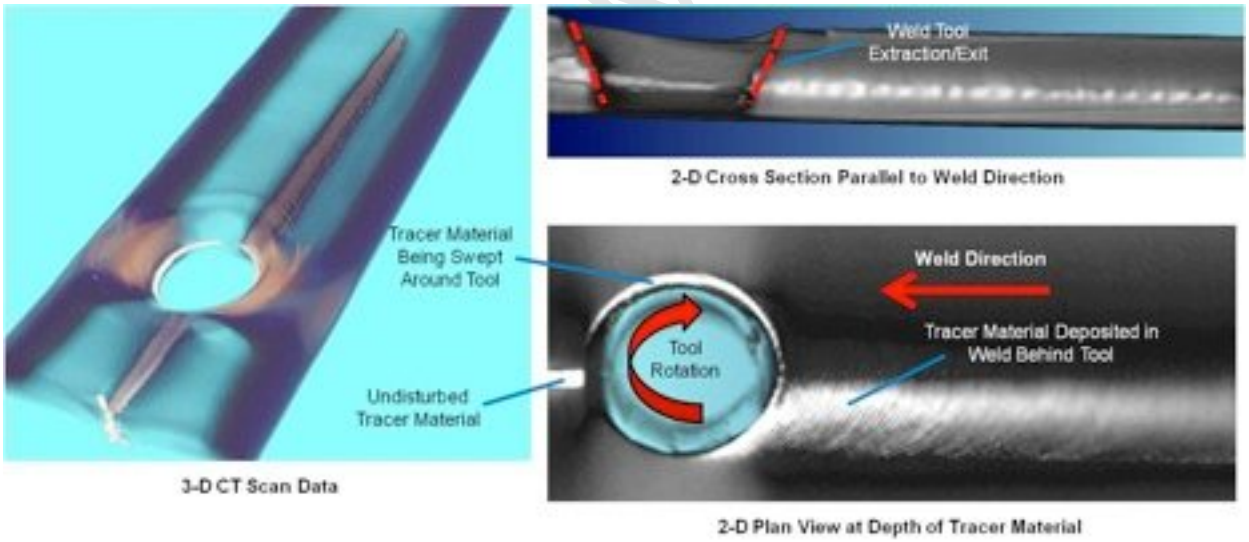

Figure 5 CT scans of a weld made at 300 RPM and 150 mm/min.

Optical macrographs from the weld cross sections, with the tracer material starting at the joint centerline, made with each of the five welding conditions tested are given in Figure 6. As seen similarly in the x-rays, the tracer material that starts at the centerline of the weld is deposited in the weld zone offset towards the advancing side of the joint. There is minimal vertical flow of material through the nugget seen in the metallographic sections, which was also observed in the CT scans. However, unlike the fairly tight distribution of the tracer material in the weld zone shown in the x-rays, the macrographs show a wider spread of the tracer material in the weld nugget, ranging from the centerline to the edge of the weld nugget. The discrepancy in difference in apparent final tracer spread within the weld nugget between the x-ray's and cross sections is due to the limited resolution of the x-ray technique compared to the metallographic evaluation. The tracer material that started in a 1.25 mm wide area was spread over an 8.5 mm wide area in the weld nugget. The height of the tracer material

band is approximately 1.25 mm, which is the same as its starting size. This is an additional indication that there is minimal vertical mixing occurring. Since the height of the tracer material remained unchanged, but its width grew by nearly 600%, the tracer material does experience some mixing with the base material. The bands of the tracer material in the nugget are due to the multiple revolutions of the tool as it passes through a given cross sectional plane along the weld length during its traverse. This shows that the structure of the weld nugget is formed by a series of layers as the tool deposits material behind it during its traverse. These observations are in agreement with the banded structures seen in x-rays and CT scans.

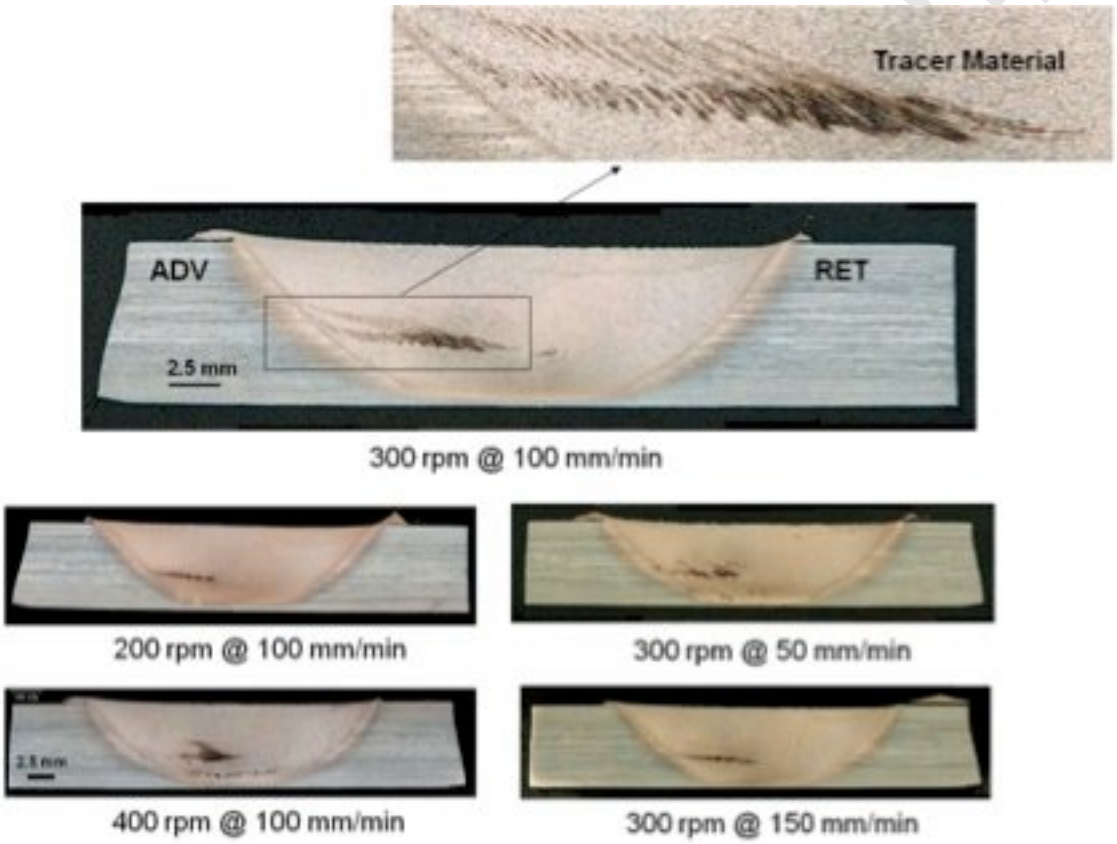

Figure 6 Macrographs of welds made under a variety of process parameters with embedded tracer material.

Even though there was no significant difference in the tracer material distributions in the center of the weld between the different welding conditions in the x-ray results, weld defect formation in the root of the joint, where there was no tracer material, was found to be strongly dependent on the welding parameters, as expected. The low rotational speed and high traversing speed conditions lead to relatively low heat inputs, which reduce material flow, prevent penetration and result in a lack of penetration defect Figure 7 a. Conversely, high rotational speed and low traversing speed conditions lead to high heat inputs, low flow stress, low process loads and thus consolidation forces, excessive stirring at the root of the joint and void defects, Figure 7 b.

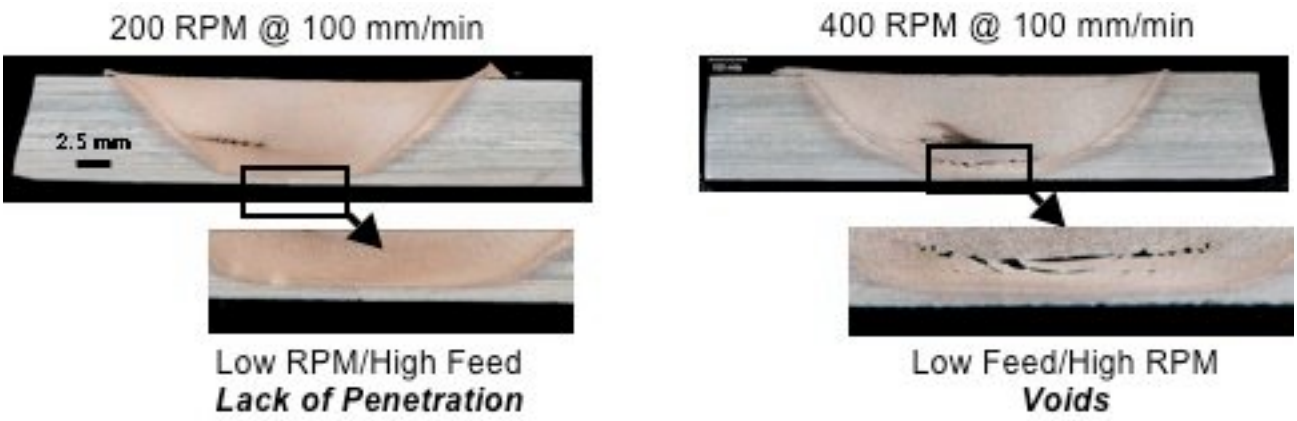

Figure 7 Cross sections of welds showing typical defects.

Discussion

The purpose of this research was to experimentally evaluate the material flow behavior during FSW of titanium, which is a subject that has been studied by several in aluminum alloys, and to gain an understanding of the relationship between processing conditions, such as traversing speed and rotational speed, on the material flow response. Two dimensional x-rays of welds showed that tracer material entering at the centerline of the weld is moved around the weld tool pin on the retreating side and then deposited behind the tool, slightly offset to the advancing side from where it started (Figure 2). It was found that material entering the weld zone on the advancing side is moved around the pin to the retreating side, pulled back behind the pin and deposited farther to the advancing side of the joint than where it started. The tracer material starting on the retreating side of the weld was moved around the pin and left on the retreating side of the joint, but still farther to the advancing side compared to where it started. This is in general agreement with the findings of Colligan (1999). However, in some cases, Colligan (1999) found that tracer material entering on the retreating side of the weld zone did remain on the retreating side of the weld and was even pushed farther to the retreating side.

High degrees of mixing are expected in aluminum welds due to the complex threaded pin tool designs used to promote high degrees of mixing (Schmidt et al., 2005). However, in titanium the pin tool is essentially featureless since any features would be destroyed quickly during the process, so minimal mixing of the tracer material with the base material was anticipated. The radiographic (Figure 2, Figure 3, Figure 4) and CT scans (Figure 5) didn't provide much evidence of the tracer material mixing with the base metal due to the lack of resolution in the imaging, but the metallographic sections did (Figure 6). In some of the cross sections, material was spread over the weld width up to 600% wider than it began in the pre-machined pocket. This was mostly a spreading across the width of the weld as there was a minimal change in the distribution of the material in the weld nugget vertically relative to how it started. Because the width of the tracer material in the weld nugget was larger than its starting condition and the height remained roughly the same, this does imply some degree of mixing occurred with the base material.

The difference in material flow patterns as a function of the process parameters shown by the two dimensional x-rays and CT scans, Figure 3, was not as significant as expected. Metallographic cross sections (Figure 6) provided more insight though. For the lowest traversing speed condition (50 mm/min) there appears to be a larger distribution of the tracer material in the vertical direction compared to the moderate traversing speed conditions implying a greater degree of mixing at slower

travel speeds. The highest rotational speed condition (400 RPM) had the least amount of tracer material spreading across the width of the weld but the most in the vertical direction. Higher rotational speeds were initially expected to lead to greater degrees of mixing, but it may be that the high rotational speeds lead to high enough temperatures that in turn lower the flow stress and coefficient of friction between the tool and weld zone material to the point that the amount of gross mixing is actually reduced. This correlates to the measured plunging forces as a function of process parameters, Table 2, where the plunging force decreased significantly with increasing rotational speed. Higher temperatures associated with a faster rotating tool generating more heat would result in lower flow stresses in the weld nugget material and lower reaction forces, or plunging forces. Traversing speed was found to have a secondary effect on plunging force, but decreased traversing speeds also lowered plunging forces as the weld tool would not be running into the cold material ahead of the weld zone as quickly. These observations are in agreement with previous research on the temperature response in titanium FSW nuggets as a function of processing parameters (Edwards and Ramulu, 2010).

By visually examining the cross sections in Figure 6 it appears that there could be some relationship drawn between the material flow and the ratio of rotational speed to traversing speed. Both the 300 RPM @ 150 mm/min and 200 RPM @ 100 mm/min conditions, that have the lowest rotational speed to traversing speed ratios, lead to similar tracer material distribution across the width of the weld cross section and minimal vertical displacement. Higher ratios of rotational speed to traversing speed ratio conditions (300 RPM @ 50 mm/min and 400 RPM @ 100 mm/min) lead to greater vertical displacement of the tracer material.

CT scans of the welds provided insight into the through thickness movement of the weld nugget material (Figure 5). Since titanium FSW tools and pins are featureless, it was not expected to see any significant vertical movement of tracer material, unlike in aluminum alloys, which use threaded tools that promote vertical material flow. However, some downward movement of the tracer material was seen. This is attributed to the forging force of the heel on the 3 degree back tilted weld tool as it passes over the material previously stirred by the pin. Due to the tool back tilt, the trailing shoulder of the tool, or the heel, presses into the weld nugget. This causes a compressive forging action that pushes the tracer material down in to the weld. This forging observation is consistent with that of previous works, such as Seidel and Reynolds (2001). The back tilted pin combined with the pin rotation could have also contributed to the downward material movement. Even though more bulk downward material movement was seen than anticipated, the vertical mixing of the tracer material with the base metal wasn't significant as discussed previously. While high quality butt joints could be obtained even with this lack of vertical mixing, this could be a challenge for making other joint types like laps.

Another finding during this study was the effect of weld parameters on defect formation in the root of the joint (Figure 7) observed via metallographic examinations as there was no tracer material embedded in the root to observes this via radiography. High heat input conditions, from high rotational speeds and low traversing speeds, lead to higher temperatures, reduced flow stresses, decreased plunging forces (15-18 kN @ 400 RPM), and cause void formation because of a lack of consolidation forces. As shown in previous research by Edwards and Ramulu (2009), when the welding conditions are "hot" the plunging force while welding in position control becomes low, relatlivy speaking, which can create voids as the plunging forces aren't sufficient for consolidating voids under the weld tool. Conversely, low heat input conditions, from low rotational speeds and high traversing speeds, lead to lower process temperatures and higher plunging forces (53-62 kN @ 200 RPM) and do not allow sufficient stirring and penetration, resulting in lack of penetration defects, meaning that neither the TMAZ nor WN penetrate all the way through the thickness of the plate. Since these welds were performed in position control, the plunging force was a response variable and not directly controlled,

but increasing the plunging force in the high heat input welding conditions may have aided in the consolidation of the void defect formation.

Finally, the CT scans, x-rays and cross sections showed that the tracer materials were deposited behind the weld tool in bands that are related to the tool feed marks on the top surface of the welds. This implies that the tool marks on the top of the welds are indicative of subsurface characteristics. The way the tracer materials were left behind the tool in a series of bands, seen both from the plan view of the weld in the x-rays and in the perpendicular metallographic cross sections, it is concluded that the weld nugget is formed by a progressive stacking of material as it is extruded and deposited from behind the weld tool, the frequency of which is equivalent to the weld pitch.

In one particularly interesting case not presented in the results section was a weld made at 300 RPM at 100 mm/min that had unstable, oscillating, plunging forces (25–28 kN) near the end of the weld (Figure 8). This was attributed to a programming error in plunge depth, but the weld was still allowed to complete. Examination of the weld surface showed uneven tool marks that are in phase with the load oscillations during the weld. X-rays and CT scans also showed that the material flow was unstable and also in phase with the load oscillations and uneven feed marks on the weld surface. This observation can help support the concept of in-process quality control. If the plunging forces are relatively stable, and the weld surface is uniform, the material flow patterns will also be stable, resulting in uniform subsurface weld quality. However, if a weld has unstable loads, or an uneven weld surface, it is expected that there are subsurface implications that should be addressed prior to accepting a weld.

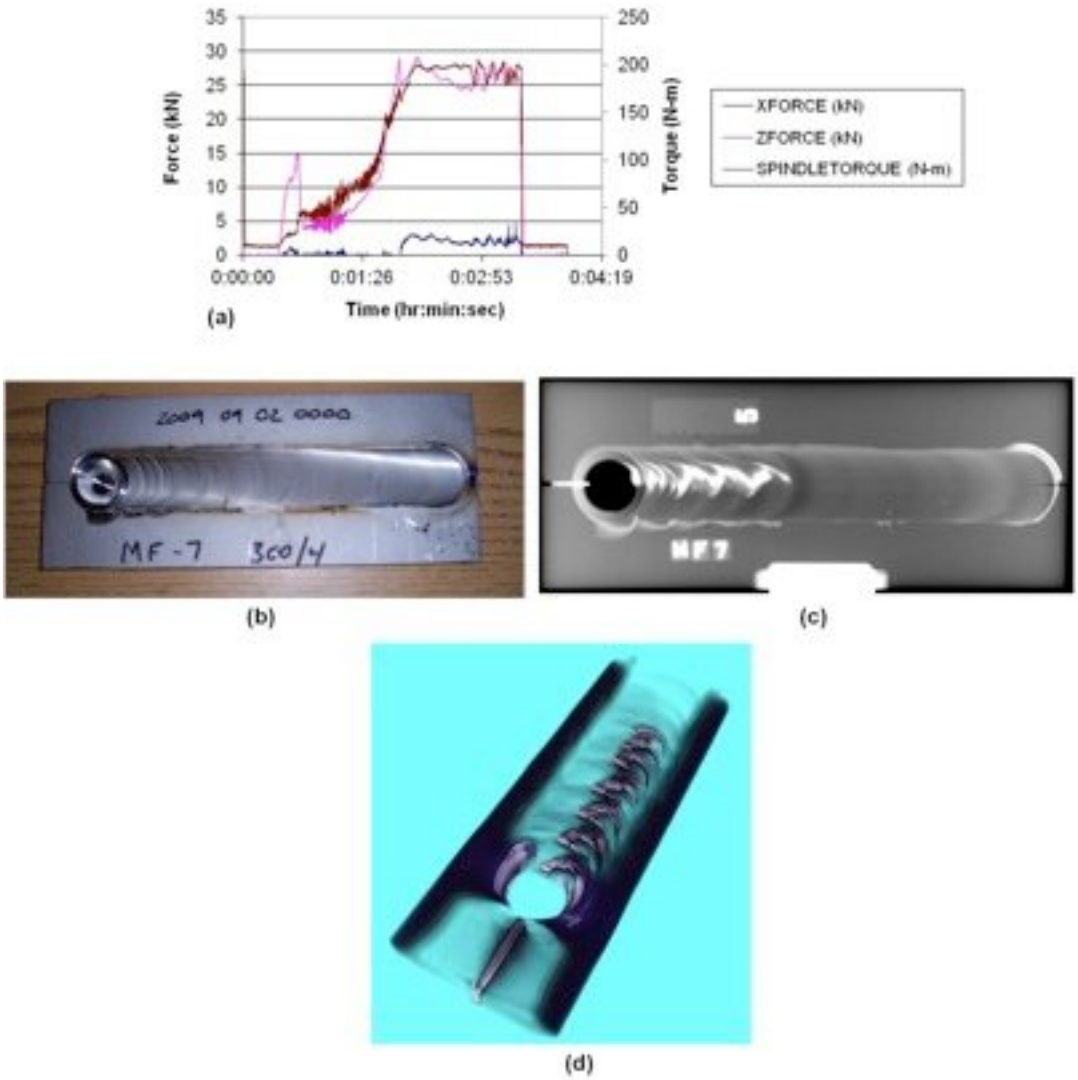

Figure 8 Effect of a) weld load oscillations on b) weld surface c) sub-surface and d) CT scan.

Conclusions

1. Material flow patterns during FSW of Ti-6Al-4V can be experimentally observed by embedding refractory alloy powder into the joint, welding through it and then inspecting the weld via radiography and/or metallographically to determine the final location of the powder relative to its starting location. This technique has been successfully used by others in aluminum alloy FSW's, but this is the first time it has been reported in titanium FSW.
2. The tracer material starting on the weld centerline was moved around the retreating side of the tool and deposited behind, towards the advancing side of the weld. The tracer material was spread over an area nearly 600% wider than it started, but did not change significantly in height. This distribution of tracer material implies some amount of mixing takes place in the weld nugget even though the weld tool is featureless.
3. No strong trends were observed between material flow behavior in the center of the weld using the tracer material and the process parameters, rotational speed and traversing speed, for the range of conditions tested via x-ray analysis. However, metallographic sectioning highlighted a potential relationship between weld conditions and material flow.

a. Low rotational speed to traversing speed ratios ("cold" welds) resulted in a wide spread of the tracer material across the width, but not the thickness.
b. High rotational speed to traversing speed ratios ("hot" welds) led to more vertical distribution of the tracer materials and in the most extreme case, minimal distribution of the tracer material across the width of the weld.
c. Weld parameters were found to affect defect formation in the bottom, or root, of the weld zone via metallographic examination as no tracer material was placed in the root. Parameters associated with high heat inputs lead to voids while low heat inputs cause lack of penetration.

4. The tool marks left on the surface of the weld are related to the sub-surface structure of the joint, the frequency of which is related to the weld pitch. The joints are formed by a successive layering of material that is deposited behind the tool. Oscillations in the plunging force will cause an inconsistent weld surface and indicate un-stable sub-surface material flow patterns. This could support implementing in-process quality control of the FSW process based on the stability of measured plunging forces. Consistent welding loads would be expected to result in consistent sub-surface characteristics, which is now currently only validated by destructive testing like metallography or non-destructive inspection such as radiography at added expense.

Acknowledgements

The authors of this paper would like to thank The Boeing Company for financially supporting this work and Rhenium alloys for donating the tungsten powder.

References

Arbegast, W., 2008, A Flow-partitioned deformation zone model for defect formation during friction stir welding, Scripta Materialia, Vol. 58, pp. 372-376.

Colligan, K., 1999, Material Flow Behavior during Friction Stir Welding of Aluminium, Supplement to the Welding Journal, pp. 229-237.

Edwards, P., Ramulu, M., 2009, Effect of process conditions on superplastic forming behaviour in Ti–6Al–4V friction stir welds, Science and Technology of Welding and Joining, Vol. 14, No. 7, pp. 669-680.

Edwards, P., Ramulu, M., 2010, Identification of the Process Parameters for Ti-6Al-4V Alloy Friction Stir Welding, Journal of Engineering Material and Technology, Vol. 132, pp. 1-10.

Edwards, P., Ramulu, M., 2010, Peak Temperatures during Friction Stir Welding of Ti-6Al-4V, Science and Technology of Welding and Joining, Vol. 15, No. 6, pp. 468-472.

Frary, M., Abkowitz, S.M., Abkowitz, S., Dunand, D.C., 2003, Microstructure and mechanical properties of Ti/W and Ti-6Al-4V/W composites fabricated by powder-metallurgy, Materials Science and Engineering A, Vol. 344, pp. 103-112.

Grobstein, T., 1990, Properties of Pure Metals, Properties and Selection: Nonferrous Alloys and Special-Purpose Materials, Vol 2, ASM Handbook, ASM International, p 1099–1201.

Guerra, M., Schmidt, C., McClure, J.C., Murr, L.E., Nunes, A.C., 2003, Flow Patters during Friction Stir Welding, Material Characterization, Vol. 49, pp. 95-101.

Klopp, W.D., Review of Ductilizing of Group VI Elements by Rhenium and other solutes, NASA TN D-4955

Li, Y., Murr, L.E., McClure, J.C., 1999, Solid-State Flow Visualization in the Friction Stir Welding of 2024 Al to 60601 Al, Scripta Materialia, Vol. 40, No. 9, pp. 1041-1046.

Mishra, R., Mahoney, M. (Eds.), 2007. Friction Stir Welding and Processing, ASM International, Ohio.

Schmidt, H.N.B., Dickerson, T.L., Hattel, J.H., 2005, Material flow in butt friction stir welds in AA2024-T3, Acta Materialia, Vol. 45, pp. 1199-1209.

Schneider, J.A., 2007, Temperature Distribution and Resulting Metal Flow. In: Mishra, R., Mahoney, M. (Eds.), 2007. Friction Stir Welding and Processing, ASM International, Ohio, Chapter 3, pp. 37-49.

Seidel, T.U., Reynolds, A.P., 2001, Visualization of the Material Flow in AA2195 Friction-Stir Welds using a Marker Insert Technique, Metallurgical Materials Transactions A, Vol. 32, pp. 2897-2884.

Tang, W., Guo, X., McClure, J.C., Murr, L.E., Nunes, A., 1998, Heat Input and Temperature Distribution in Friction Stir Welding, Journal of Material Processing and Manufacturing Science, Vol. 17, pp. 163-172.

Yih, S., 1990, Propeties of Pure Metals, Properties and Selection: Nonferrous Alloys and Special Purpose Materials, Vol. 2, ASM Handbook, ASM International, p 1099-1201.

List of Tables

Table 3 Summary of parameters used for material flow experiments.

Weld #	Rotational Speed (RPM)	Traversing speed (mm/min)	Tracer Location
1	300	100	CL
3	400	100	CL
4	300	50	CL
5	300	150	CL
6	200	100	CL
8	300	100	Ret
9	300	100	Adv

Table 4 Experimentally measured plunging forces as a function of FSW process parameters.

Rotational Speed (RPM)	Traversing speed (mm/min)	Plunging force (kN)
300	50	22-24
300	100	26-29
300	150	36-40
200	100	53-62
400	100	15-18